ARO 18188.3-EG

(2)

AD-A168 948

DIESEL CYLINDER GAS-SIDE HEAT FLUX TO A CERAMIC SURFACE

FINAL REPORT

GARY L. BORMAN AND J. C. HUANG

JUNE 1, 1986

DTIC
ELECTE
JUN 25 1986
S D
D

U.S. ARMY RESEARCH OFFICE
CONTRACT NUMBER
DAAG29-81-K-0082

UNIVERSITY OF WISCONSIN-MADISON
1500 JOHNSON DRIVE
MADISON, WI 53706

DTIC FILE COPY

APPROVED FOR PUBLIC RELEASE
UNLIMITED DISTRIBUTION

THE VIEW, OPINIONS, AND/OR FINDINGS CONTAINED IN THIS REPORT ARE THOSE OF THE AUTHOR(S) AND SHOULD NOT BE CONSTRUED AS AN OFFICIAL DEPARTMENT OF THE ARMY POSITION, POLICY, OR DECISION, UNLESS SO DESIGNATED BY OTHER DOCUMENTATION.

UNCLASSIFIED

SECURITY CLASSIFICATION OF THIS PAGE (When Data Entered)

REPORT DOCUMENTATION PAGE

READ INSTRUCTIONS BEFORE COMPLETING FORM

1. REPORT NUMBER ARO 18188.3-EG	2. GOVT ACCESSION NO. N/A	3. RECIPIENT'S CATALOG NUMBER N/A
4. TITLE (and Subtitle) DIESEL ENGINE CYLINDER GAS-SIDE HEAT FLUX TO A CERAMIC SURFACE		5. TYPE OF REPORT & PERIOD COVERED FINAL 5/18/81 - 6/30/85
		6. PERFORMING ORG. REPORT NUMBER
7. AUTHOR(s) Gary L. Borman Jeffrey C. Huang		8. CONTRACT OR GRANT NUMBER(s) DAAG29-81-K-0082
9. PERFORMING ORGANIZATION NAME AND ADDRESS Engine Combustion Laboratory University of Wisconsin-Madison 1500 Johnson Dr., Madison, WI 53706		10. PROGRAM ELEMENT, PROJECT, TASK AREA & WORK UNIT NUMBERS from 1634 - 1498
11. CONTROLLING OFFICE NAME AND ADDRESS U. S. Army Research Office Post Office Box 12211 Research Triangle Park, NC 27709		12. REPORT DATE June 1, 1986
		13. NUMBER OF PAGES 38
14. MONITORING AGENCY NAME & ADDRESS (if different from Controlling Office)		15. SECURITY CLASS. (of this report) Unclassified
		15a. DECLASSIFICATION/DOWNGRADING SCHEDULE

16. DISTRIBUTION STATEMENT (of this Report)

Approved for public release; distribution unlimited.

17. DISTRIBUTION STATEMENT (of the abstract entered in Block 20, if different from Report)

NA

18. SUPPLEMENTARY NOTES

The view, opinions, and/or findings contained in this report are those of the author(s) and should not be construed as an official Department of the Army position, policy, or decision, unless so designated by other documentation.

19. KEY WORDS (Continue on reverse side if necessary and identify by block number)

Diesel Combustion, Heat Transfer, Adiabatic Engine, Radiation, Convection, Ceramic.

20. ABSTRACT (Continue on reverse side if necessary and identify by block number)

SEE OTHER SIDE

DD FORM 1473 1 JAN 73 EDITION OF 1 NOV 65 IS OBSOLETE

UNCLASSIFIED

SECURITY CLASSIFICATION OF THIS PAGE (When Data Entered)

Results of four research projects each dealing with instantaneous heat flux to the cylinder head of a reciprocating engine are given. The projects are: heat flux measurements in a diesel engine with variations in injection pressure, nozzle tips and swirl; development of instrumentation for radiation measurements in a diesel cylinder; heat flux measurements to various surfaces on the head of a diesel engine including a normally cooled metal surface, an insulated metal surface and a zirconia surface; and initial attempts to simultaneously measure the fluid motion and heat flux in a motored engine boundary layer.

The variation of injection pressure nozzle tips and swirl in a direct injection diesel showed strong coupling between combustion and heat flux. Variations in swirl can affect combustion so strongly that normally observed trends of increased heat flux with increased swirl can be reversed.

An instrument for radiation measurement which uses a wall jet to reduce convection is described. It is shown that the compression of the jet by the combustion heat release prevents zeroing of the convection. Future development of the instrument depends on finding a method to correct for this variation in convective flux. Other methods of direct radiation measurement are briefly discussed.

The major portion of the research was devoted to heat flux measurements to the surface of an instrumentation plug in the head of a single cylinder TACOM-LABECO diesel. Comparisons made between data for insulated and uninsulated surfaces show that the hot metal surface gave reduced time averaged heat transfer, but gave a higher peak heat flux than a normally cooled surface. Data for a zirconia plate surface showed a reduction in peak flux which was larger than predicted from the rise in surface temperature alone. The differences observed for both the insulated metal and ceramic surfaces are attributed to changes in radiation flux caused by changes in deposit and surface properties.

FOREWARD

This report covers the work done on diesel engine heat transfer and consists of four parts. The first part is a study of the effects of fuel injection parameters and swirl on instantaneous heat transfer rates to the head of an open chamber TACOM-LABECO engine. The results of this study were published in a 1985 SAE paper and thus will be only briefly reviewed here. The second part is a study of the effects of extent of cooling and wall surface properties on instantaneous heat transfer to a surface in the head of a fired TACOM-LABECO engine. Results for three surfaces were obtained; a cooled metal surface, an insulated metal surface and a zirconia plate. Instrumentation of a plate with sprayed-on zirconia was attempted, but was not successful. A paper and Ph.D. thesis based on this work are in preparation. Thus a more complete discussion of these results is presented here. The third part is an exploratory study of radiation instrumentation methods. This work will not be published as the instrument concepts proved worthwhile, but considerable work would be required, beyond the scope of the grant, to further develop the idea. Some comments are made concerning additional developments of other instruments which resulted from the grant study, but have not yet produced data. Part four discusses our preliminary work on a basic experimental study of the coupling between local fluid flow and heat flux in a hot motored engine. This study was our first attempt to use a two component LDV system obtained from a DOD equipment grant. Major problems were encountered with the coupling between the LDV and the data processing system. This initial work resulted in an MS thesis. Continuation of this study is currently being funded by TACOM.

QUALITY INSPECTED 3

A-1

TABLE OF CONTENTS

LIST OF ILLUSTRATIONS AND TABLES

PART I

Injection and Swirl Effects on Diesel Heat Transfer

This study was done jointly by two Ph.D. students, J. Van Gerpen and C. Huang. The heat transfer portion was carried out by Mr. Huang as part of the grant work. In this study a TACOM-LABECO engine was fitted with a special head which allowed placing two surface thermocouples in the head, one over the combustion bowl and one over the squish area. The head was also designed to allow use of an American Bosch electronic fuel injector. The primary parameters varied were: injection pressure, number and size of holes, and swirl ratio. The results are reported in SAE paper 850265. Some of the major results regarding the heat transfer are summarized below.

Data taken with the 4-hole nozzle show similar trends versus the operating parameters. This could be expected since the two 6-hole nozzles are similar in size and geometry, and the locations of the upstream fuel sprays closest to the heat flux transducers were the same for the 6 and 4 hole nozzles.

The two heat flux transducers, STC1 and STC2, which are located in the engine head over the piston bowl and piston squish lip, respectively, show similar trends of data versus all the operating parameters. However, heat fluxes and surface temperatures at STC1 are significantly higher than those at STC2. Though the two transducers are only 14 mm apart, differences of 20° to 30°C in time-averaged surface temperature were observed even though internal cooling was applied to the cylindrical instrumentation plug in an effort to better approximate the condition of one-dimensional conduction. Also, peak surface heat fluxes at STC1 are typically two to three times those at STC2.

These observations have clearly demonstrated the nonuniformity in spatial distribution of diesel in-cylinder heat-transfer.

The peak heat flux increases and becomes more advanced with increasing injection pressure. This is due most likely to the increased amount and rate of premixed burning as well as the higher rate of early mixing controlled burning at high injection pressures. The time-averaged heat flux generally increases with the increasing injection pressure.

Both the time-averaged and peak values of the surface heat flux decrease, but the peak timing of surface flux advances with increasing swirl level. The increased heat flux with the increasing swirl is observed before injection, but the trend with the swirl is reversed when combustion starts. This effect of swirl on heat flux during combustion can be explained by the limited fuel spray penetration with increased swirl and the movement of the fuel spray relative to the transducers.

The comparison of local surface heat flux data with the heat release calculated by Van Gerpen (1) again shows the effect of movement of the fuel spray with air swirl relative to the transducers. The sudden rise in the flux correlates well at high swirl, but is retarded at low swirl with respect to time of ignition. The transition from premixed to mixing controlled burning is not observable on the heat flux curves.

The deficiencies of calculating the heat transfer coefficients from the experimental local heat flux data and the difference between the mass-averaged gas temperature and local surface temperature are obviously shown as the result of phase differences between the bulk gas and the local heat flux. Unsatisfactory comparisons of the experimental flux data with those calculated from the widely-used in-cylinder heat-transfer correlations demonstrate that

more detailed modeling of both the combustion and fluid mechanics are needed for improvements in such correlations.

PART II

Effects of Insulation and Surface Properties on Diesel Heat Transfer

The objective of this project was to examine the effects of various insulating techniques on surface heat flux without influencing the combustion or flow in the diesel engine. If the entire engine is insulated the volumetric efficiency and combustion will be changed thus confounding the surface material effects. Of course heat transfer measurements in an insulated engine will also be required, but such measurements were not a part of the ARO funded work.

The concept of the experiment was achieved by designing a special head for a TACOM-LABECO engine. This head and engine are different from the ones discussed in Part I of this report. Figure 1 shows the plan view of the head. The special instrumentation port contains a plug, the bottom surface of which makes up a portion of the gas side cylinder head surface. This plug was modified in design to allow measurements from an insulated and uninsulated (cooled) metal surface and a zirconia plate. Figures 2 and 3 show the instrumentation plug assemblies with the insulated metal plate and zirconia plate, respectively. A plug was also constructed for use with a sprayed zirconia surface, but the instrumentation was not successful.

In all cases, thin film thermocouples mounted at the positions STC1 and STC2 of Figure 1 were used to measure the instantaneous surface temperature. Comparison of measurement results at the two locations would show the effect of a non-isothermal upstream condition. Conventional coaxial type Bendersky

surface thermocouples (2) with J-type materials were used for the metal surface tests. Several different arrangements of backside junctions were attempted. These second junctions are needed in order to calculate the steady state component of the flux. The use of three second junctions spaced around the center wire of the coaxial surface thermocouple allowed correction for non-one-dimensional heat flow between the surface and the second junction. For the zirconia plate overlapping rhodium and platinum thin films each connected to a wire were used to form the couple. Figure 4 shows the arrangement. Experiments were conducted with a pulsed laser to determine if the overlapping junction was responding. It appears that not all areas of the supposed junction respond, however steady state oven tests gave a good correlation with temperature.

The work was interrupted midway by an engine rebuild which involved replacement of the scored liner and piston. The piston cup geometry was at that time redesigned for better match to fuel spray penetration and to lower the compression ratio from 22:1 to 17:1 to allow operation at more appropriate boosted intake conditions. The insulated versus uninsulated metal study was conducted before the engine rebuild. The standard operating condition parameters for this study are shown in Table 1. The zirconia versus uninsulated metal study was carried out after the engine rebuild. Parameters for the standard operating condition are shown in Table 2. The uninsulated metal (baseline) data were collected both before and after the engine rebuild. The experimental matrix is shown in Table 3.

Fortyfive and 200 consecutive cycles of surface temperature data were taken at the rate of every 0.5°CA for the insulated versus uninsulated metal and the zirconia versus metal case, respectively. The surface temperature data were ensemble-averaged and analyzed following the procedures outlined by

Overbye et al. (3) for the calculation of surface heat flux. The assumptions of constant wall thermal properties and 1-D heat transfer were made. For the insulated metal case, the steady state heat flux had to be calculated assuming zero instantaneous surface flux at the time of zero gas-wall temperature difference during compression, as suggested by Sihling and Woschni (4), since the backside thermocouple failed.

Figure 5 shows the effect of metal plate back-side insulation on surface temperature. With insulation, the time-averaged surface temperature increased from 115° to 205°C as the equivalence ratio changed from 0.3 to 0.6. The increase in surface temperature swing is 65% to 35% over the same range of equivalence ratio. Peak timing for the surface temperature is 2 to 3°CA more advanced for the insulated case. Figure 6 shows the comparisons of peak surface heat flux and time-averaged heat flux for the insulated and uninsulated metal. Insulation increases the peak surface heat flux by 70% and 5% at 0.3 and 0.6 equivalence ratio, respectively. The reduction in time-averaged heat flux due to insulation increases from 10% at 0.3 to 30% at 0.6 equivalence ratio. It is believed that the surface soot deposit was reduced due to elevated surface temperatures, causing increased peak values of the flux and more advanced timings of the peaks. The increased average surface temperature is responsible for the reduction in time-averaged heat flux for the insulated case. Figure 7 shows the comparison of cyclic surface heat fluxes for the insulated and uninsulated metal. Insulated metal surface heat fluxes are characterized by the double-humped appearance for the 125° and 230° shrouded position. For the 185° shroud position at which minimum swirl was generated, surface heat fluxes do not have two humps. The double-humped shape of the ensemble-averaged surface flux is typical of that for the individual cycle. Also, the magnitude of the first hump monotonically increases with the

equivalence ratio. It is thus believed that this double-humped characteristic of fluxes is related to combustion , or the fuel spray movement with swirl.

Figure 7 shows that the insulated case surface heat flux has larger negative values during the early compression and late expansion stroke. Not shown in the figure for the insulated case is the larger negative flux during the intake stroke. These larger negative surface fluxes for the insulated case are the result of higher surface temperature. These negative fluxes during intake process may result in reduced volumetric efficiency. Even though the small area of insulation used in this study has no observable effect on engine performance and combustion characteristics, a full scale cylinder insulation can be expected to cause significant reduction in volumetric efficiency.

Figure 8 shows the comparisons of time-averaged values and swing magnitudes of the surface temperatures for the zirconia and uninsulated metal. The time-averaged surface temperature for zirconia rose from 100° to 170°C as the equivalence ratio increased from 0.3 to 0.5. The magnitude of the surface temperature swing for the zirconia is 1.9 to 2.4 times that for the metal over the same range of equivalence ratio. Figure 9 shows a comparison of the surface temperature histories for the zirconia and metal.

Figure 10 shows the comparisons of the peak and time-averaged values of surface heat fluxes for the zirconia and uninsulated metal. The time-averaged heat flux for zirconia is 33% less at 0.3 equivalence ratio, and is about 40% less at 0.4 and 0.5 equivalence ratio. Note that these reductions in time-averaged fluxes are 10 to 15% more than those achieved by the insulated metal. But the time-averaged flux values for the insulated case were calculated, so that direct comparisons may not be valid. Peak values of the surface fluxes for zirconia are only 45 to 50% of those for the uninsulated

metal. Figure 11 shows the comparison of cyclic surface heat fluxes for the zirconia and metal.

The 50 to 55% reduction in peak surface heat fluxes for the zirconia may be associated with two factors. Firstly, the higher surface temperature of zirconia may result in a lower convective flux. An estimate based on the mass-averaged gas and wall temperature difference shows that the peak convective heat flux for zirconia is about 20% less than that for metal. Secondly, the sparsely sooted surface of zirconia may have a lower emissivity than the heavier sooted surface of uninsulated metal. In the radiant heat flux measurement conducted by Oguri and Inaba (5) in an open chamber diesel engine, a sooted metal surface received radiant fluxes with 40 to 80% higher peak values than a clean metal surface. Such differences were attributed to the increased surface emissivity of the sooted surface. Though surface emissivities of the zirconia and uninsulated metal surfaces are not actually known, visual inspections indicate that the zirconia surface may have a lower emissivity due to its sparse surface soot deposit. Since the peak radiant heat flux may be as much as 50% of the instantaneous surface flux, such a reduction in radiant flux may result in significant reduction in surface flux.

Figure 11 shows that the uninsulated metal surface heat flux has larger negative values during the early compression and late expansion stroke. Not shown in the figure is the fact that the uninsulated metal gave a slightly larger negative flux during the intake stroke. This observation seemingly indicates that for the same amount of cylinder insulation with zirconia, the volumetric efficiency may be slightly improved over the conventionally cooled case. This contradicts the volumetric efficiency comparisons between the zirconia-insulated and normally cooled case (6,7). However, several factors have to be considered when making such a comparison. The zirconia plate

surface temperatures in this study are significantly lower than those projected for the production type engines at rated conditions due to the low engine speed and light loads. Also, the uninsulated plug assembly was not cooled internally, and thus may have slightly higher surface temperature than the rest of the cylinder surface area. These two factors may have contributed to smaller differences in observed surface temperatures and the reversed trend in projected volumetric efficiency. However, based on the comparison between Figures 7 and 11, a valid conclusion may be made that a zirconia-insulated engine can achieve higher volumetric efficiencies than a conventional engine operated at the same surface temperature levels.

Figure 12 shows the comparison between data at STC1 and STC2. The close comparison suggests that the effect of cooler surface temperatures upstream of the plug may be diminished by the time the flow reaches the upstream transducer. The measurement results are thus believed to be free of the effects of non-isothermal upstream conditions.

Based on the estimate of temperature-dependent thermal property variations made by Morel et al. (8), the assumption of constant thermal properties in the calculation of surface heat flux should be valid for the small amount of cyclic temperature fluctuations experienced in this study. The magnitude of surface temperature swings for zirconia is not as high as predicted from the thermal properties comparison with the metal due to the large reduction in the surface heat flux. It is thus believed that the concern of thermal shock failure of zirconia parts due to cyclic thermal loading under similar operating conditions may be less than previously anticipated.

The only observable crack in the zirconia plate after 12 hours of engine firing is a hairline crack extending from one of the connecting wire holes for

STC2 to the closer edge of the plate. The crack is well terminated and the plate backside expoxy seemed to still be effective. The crack might have been initiated from a manufacturing flaw and may have developed during a large change in load.

Table 1

Standard Operating Condition for the

Insulated versus Uninsulated Metal Study

Speed	1000 RPM
Injection Timing	22°CA BTDC
Compression Ratio	22:1
Equivalence Ratio	0.5
Intake Condition	Naturally Aspirated
Intake Valve Shroud Position	125°

Table 2

Standard Operating Condition for the

Zirconia versus Uninsulated Metal Study

Speed	1000 RPM
Injection Timing	15°CA BTDC
Compression Ratio	17:1
Equivalence Ratio	0.5
Intake Pressure	1.5 atm. absolute
Intake Temperature	65°C
Intake Valve Shroud Position	125°

Table 3
Experimental Matrix for the Study of Heat-Transfer to a Ceramic Surface

I. Insulated vs. Uninsulated Metal

Measurement at STC1 and STC2.

A. Insulated Metal

1. Naturally Aspirated; 125°, 185°, 230° Shroud Position; $\Phi = 0.3, 0.4, 0.5, 0.6$
2. Boosted Intake; 230° Shroud Position; $\Phi = 0.3$.

B. Uninsulated Metal

1. Naturally Aspirated
   a. 125° Shroud Position; Forced Air Cooling on Back-Side, Uncooled Back-Side; $\Phi = 0.3, 0.4, 0.5, 0.6$
   b. 185° Shroud Position; $\Phi = 0.3, 0.4, 0.5$.
2. Boosted Intake; 125°, 185° Shroud Position; $\Phi = 0.3, 0.4, 0.5$.

II. Zirconia vs. Uninsulated Metal

A. Zirconia

1. Measurement at STC1 and STC2.
   125°, 230° Shroud Position; $\Phi = 0.3, 0.4, 0.5$, and Motored (Naturally Aspirated).
2. Measurement at STC1 Only.
   230° Shroud Position; $\Phi = 0.3, 0.4, 0.5$, and Motored (Naturally Aspirated).

B. Uninsulated Metal

Measurement at STC2 only.
125° Shroud Position; $\Phi = 0.3, 0.4, 0.5$, and Motored (Naturally Aspirated).

PART III

Radiation Instrumentation

Radiation in the diesel engine takes place primarily by the mechanism of soot radiation. Radiation starts near the end of the premixed combustion phase as the flames surround the fuel sprays and reduce the supply of air to the spray plumes. The peak of the radiation pulse is about one half of the peak heat flux. However, the radiation flux falls off rapidly so that the portion of heat rejection caused by radiation is only 20-30%. However, measurement of this flux is very important, because the radiation directly affects the combustion and the oxidation of the particulates in the cylinder. For the insulated engine the radiation flux may represent the major portion of the heat rejection. However, measurement is difficult and all attempts to measure radiation in the engine have had major flaws. In all cases the radiation has been measured through a window so that only a portion of the hemispherical value is measured. To obtain the total value from such measurements requires a large correction factor. It is possible for the correction to incorporate a serious error since nothing is known about the directional distribution. A second problem is to keep the window clean. Typically this problem has been solved by running the engine for very short periods of time. A third problem is the effects of deposits which always cover the engine surfaces. Such deposits change the radiative properties of the surface in a unknown way. Given these various problems, it was the objective of the present work to design and test new radiation instruments. In particular, a new concept using a wall jet was to be explored.

The wall jet concept was based on the cooling method often used in gas turbine combustors. A slot in the wall directs a jet of air along the wall surface. The air jet temperature is close to that of the wall so that convective heat transfer is greatly reduced. Thus with essentially zero convection, the heat flux measured at the surface is only the radiation flux.

To apply the wall jet concept to an engine it was necessary to create a pulsed jet. The concept was to direct a pulsed jet of air over a surface thermocouple during a part of the radiation flux period. Calculation of the heat flux would then give only the radiation flux. The advantage of this method is that the total radiation is measured, without geometric correction and under steady state engine conditions. If a deposit is present the thermocouple measures the flux to the wall surface, not the flux to the deposit surface. This limitation is the same as exists for total heat flux measurements when a deposit covers the thin film couple.

Considerable work was done on the basic design of the pulsed jet. A modified GMRL sampling valve was used to meter the air flow over the surface. This valve is fast acting so that the pulse can be varied from 1 ms to many milliseconds. The minimum pulse width was thus from 5-15 crank degrees. The air flow from the pulse must be directed along the wall surface by a slot or deflector. Design of the deflector for steady state flow is possible by use of the correlations developed for gas turbine combustors. However no empirical formulas are available for engine conditions or unsteady flow.

In order to test the design it is necessary to have no radiation so that the convective reduction can be determined. To approximate this requires an engine with nonluminous combustion such as a spark-ignited premixed engine. It was thus decided to mount our apparatus in the head of a Briggs and

Stratton engine. This engine has the advantage of a large available head area, but has the disadvantage of low compression and low peak pressure.

A series of tests were run using the modified GMRL valve with deflector and a surface thin film thermocouple. The calculation of the heat flux was accomplished by use of a direct analogue RC circuit method. This method has the advantage of low signal to noise and immediate read-out of the flux data. The apparatus was designed, set-up and tested by David Boggs. The basic set-up is shown in Figure 13. Comparisons could be made between the jet and no jet data so that the reduction in flux could be obtained directly. Data were obtained for various air flow rates and air pulse durations. Figure 14 shows a result for an optimum setting. The flux was reduced by about 70%, however the reduction beyond this point was impossible because of the compression of the boundary layer gas as the pressure in the cylinder changed due to combustion. The tests were also flawed by the presence of the flame front. More recently we have developed a flameless method of lean premixed combustion which would provide a much better test medium.

If the wall jet instrument is to ever work, it will require a correction factor to account for the non-zero convection caused by compression of the wall jet. It is possible that such data could be collected by use of the flameless-combustion-engine or by use of methanol in a diesel engine. Neither of these options were available during the contract and thus other direct methods of calibration were sought.

If calibration is to be done directly in a diesel the radiation must first be measured by some other means. Of course the existence of such means could reduce the need for the wall jet instrument.

Several methods of measurement behind windows were explored. In all cases it was found that the window must be recessed to prevent sooting of its

surface. For loads below 0.4 equivalence ratio it was found that a small recess could keep the window clean for extended periods. A better design was finally developed which incorporates a sapphire rod held at the far end and with its cylinder-side end adjacent to a small orifice. Hot gas moving through the orifice and over the rod keeps the window clean at steady state engine conditions. The theory of this design is that the window must stay hot to keep the soot from sticking to the surface and the window surface must be exposed to a rapid flow of air to blow-off the soot as it is formed. This design is presently being used in our lab to measure soot temperature and concentration by the two color method. However, when used as a total radiation instrument, the design suffers from the required large geometric correction factor.

During the last year of the grant two other methods of radiation instrumentation were investigated. They both depend on keeping the window very clean by keeping it very hot. In the first design the window is a specially shaped lens which allows the total hemispherical radiation to be gathered and measured by a detector. This instrument is currently being developed by our instrument systems center (Associate Director Gene Nutter). The second method involves measurement in three directions by three very small sapphire rods which stick-out at different angles into the chamber. The rods are brazed to hold at one end and thus act as fins. Because of their small diameter and low conductivity the rod tip surfaces will be very hot. This instrument was developed under the grant by I. Samy Mohammad. The final design involved development of the brazing technology and many other difficult design factors. The instrument is currently being fabricated but could not be completed in time to be tested under the grant funding.

The instrumentation development projects for radiation involve direct radiation measurement, but questions also remain concerning the interaction between radiation and ceramic surfaces to be used in low cooled engines. It is not yet clear how radiation and convective flux can be separated for such semi-transparent surfaces.

PART IV

Coupling of Fluid Flow and Heat Flux

The basic objectives of the parts I, II and III were to obtain heat flux data under engine conditions. However such data do not give a direct link between the convective flux and the fluid flow which controls the boundary layer. As noted in Parts I and II, the boundary layer exhibits effects which can only be due to the formation of maxima or minima in the boundary layer temperature profiles. Such behavior, plus the complicated fluid flow in the engine, must nevertheless be understood if multidimensional fluid modeling is to successfully complete heat transfer.

During the last year of the grant a two component LDV was purchased under a DOD instrumentation grant. This LDV was set-up in an attempt to obtain air velocity data in the vicinity of a surface thermocouple mounted in the modified head of a CFR engine under hot motoring conditions. Considerable problems were encountered in obtaining reasonable data rates from the LDV. A basic problem was the inability to use the "FASTRACK" (ADAC CORP.) data system in conjunction with the LDV system.

Nevertheless, the setting up and running of the system allowed for a much needed learning period. Altnough Mr. Hofeldt was unable to obtain usable data he did pave the path for the current expansion of this project under TACOM

funding. Professor J. Martin who joined our faculty last fall, after the end of this contract, has been able to solve the data rate problem by the purchase of a dedicated minicomputer.

LIST OF PUBLICATIONS

Articles

J. Van Gerpen, J. Huang and G. Borman; "The Effects of Swirl and Injection Parameters on Diesel Combustion and Heat Transfer", SAE Paper 850265, SAE Trans. Vol. 84, 1985.

J. Huang and G. Borman; "Measurement of Instantaneous Heat Flux to Metal and Ceramic Surfaces in a Diesel Engine Cylinder", submitted for presentation at the 1987 SAE Congress.

G. Borman and K. Nishiwaki; "A Review of Internal Combustion Engine Heat Transfer", to be published in Advances in Energy and Combustion Science, in press.

Theses

Jon Van Gerpen, Ph.D. Thesis, 1984. "The Effects of Air Swirl and Fuel Injection System Parameters on Diesel Combustion".

David L. Hofeldt, M.S. Thesis, 1985. "Some Preliminary Results from Heat Transfer and Velocity Measurements Near an Insulated Head in a Spark Ignited Engine".

Jeffrey Cheng-wen Huang, Ph.D. Thesis, 1986. "Diesel Engine Cylinder Gas-Side Heat Transfer to a Ceramic Surface.

LIST OF PARTICIPANTS

G. L. Borman, Professor.

D. L. Boggs, currently a Ph.D. student at Madison.

D. L. Hofeldt, M.S. student, currently Ph.D. student at Stanford University, Palo Alto, CA.

J.C. Huang, a Ph.D. student, graduating June 1986.

I. Samy Mohammad, Ph.D. student in progress, supported by Egyptian Government Fellowship.

J. Van Gerpen, Ph.D. student, now on faculty at Iowa State University, Ames, Iowa.

BIBLIOGRAPHY

1. Van Gerpen, J., "The Effects of Air Swirl and Fuel Injection System Parameters on Diesel Combustion," Ph.D. Thesis, Mechanical Engineering Department, University of Wisconsin-Madison, 1984.
2. Bendersky, D., "A Special Thermocouple for Measuring Transient Temperatures," Mechanical Engineering, Vol. 75, 1953, p. 117.
3. Overbye, V., Bennethum, J., Uyehara, O., and Myers, P., "Unsteady Heat Transfer in Engine," SAE Transactions, Vol. 69, pp. 461-493.
4. Sihling, K., and Woschni, G., "Experimental Investigation of the Instantaneous Heat Transfer in the Cylinder of a High Speed Diesel Engine," SAE Paper 790833, 1979.
5. Oguri, T., and Inaba, S., "Radiant Heat Transfer in Diesel Engines," SAE Paper 720023, 1972.
6. Hoag, K., Brands, M., and Bryzik, W., "Cummins/TACOM Adiabatic Engine Program, SAE Paper 850356, 1985.
7. Moore, C.H., and Hoehne, J.L., "Combustion Chamber Insulating Effect on the Performance of a Low Heat Rejection Cummins V-903 Engine," SAE Paper 860317, 1986.
8. Morel, T., Keribar, R., and Blumberg, P., "Cyclic Thermal Phenomena in Engine Combustion Chamber Surfaces," SAE Paper 850360, 1985.

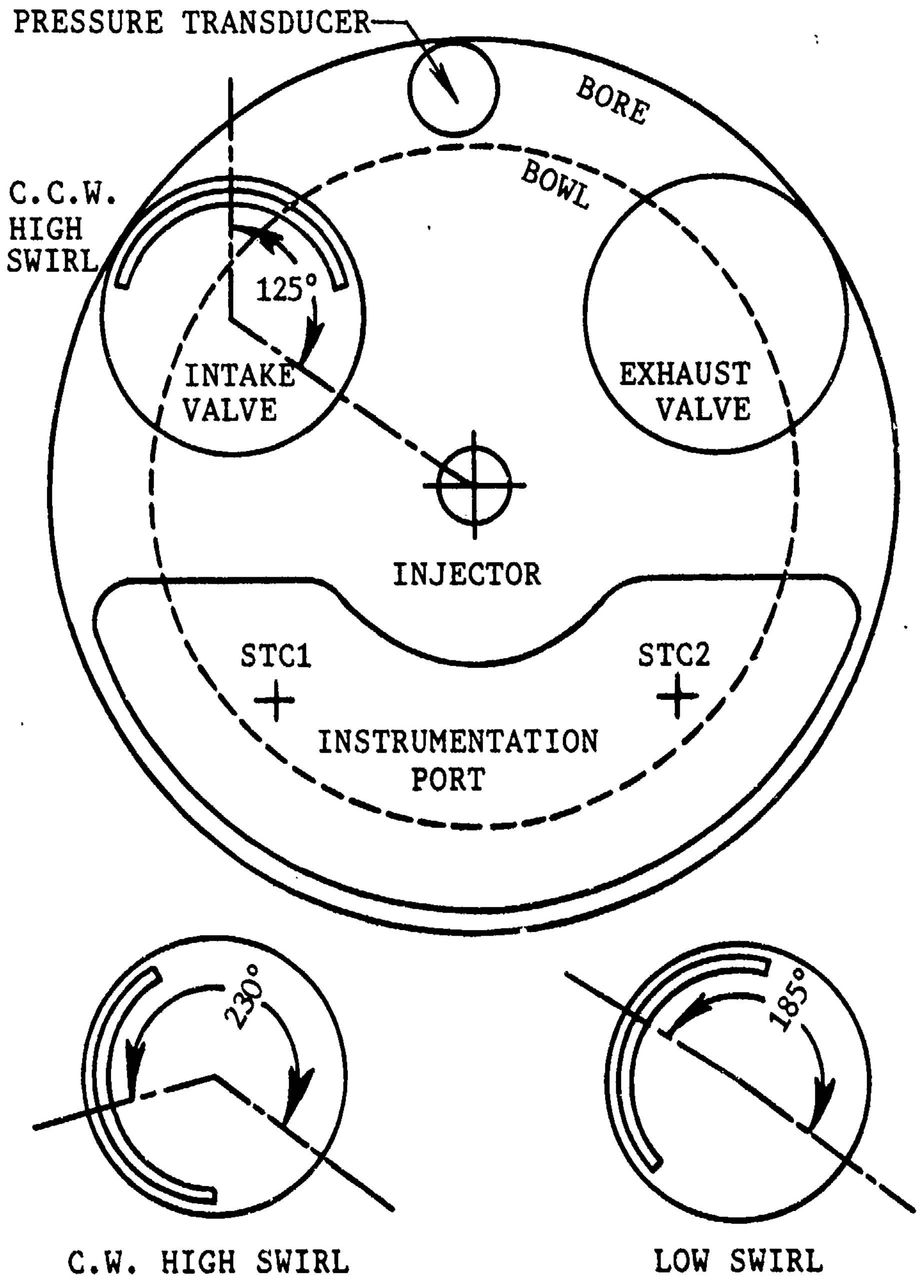

Figure 1. Locations of the Instrumentation Port and Heat Flux Transducers and the Three Positions of the Intake Shroud

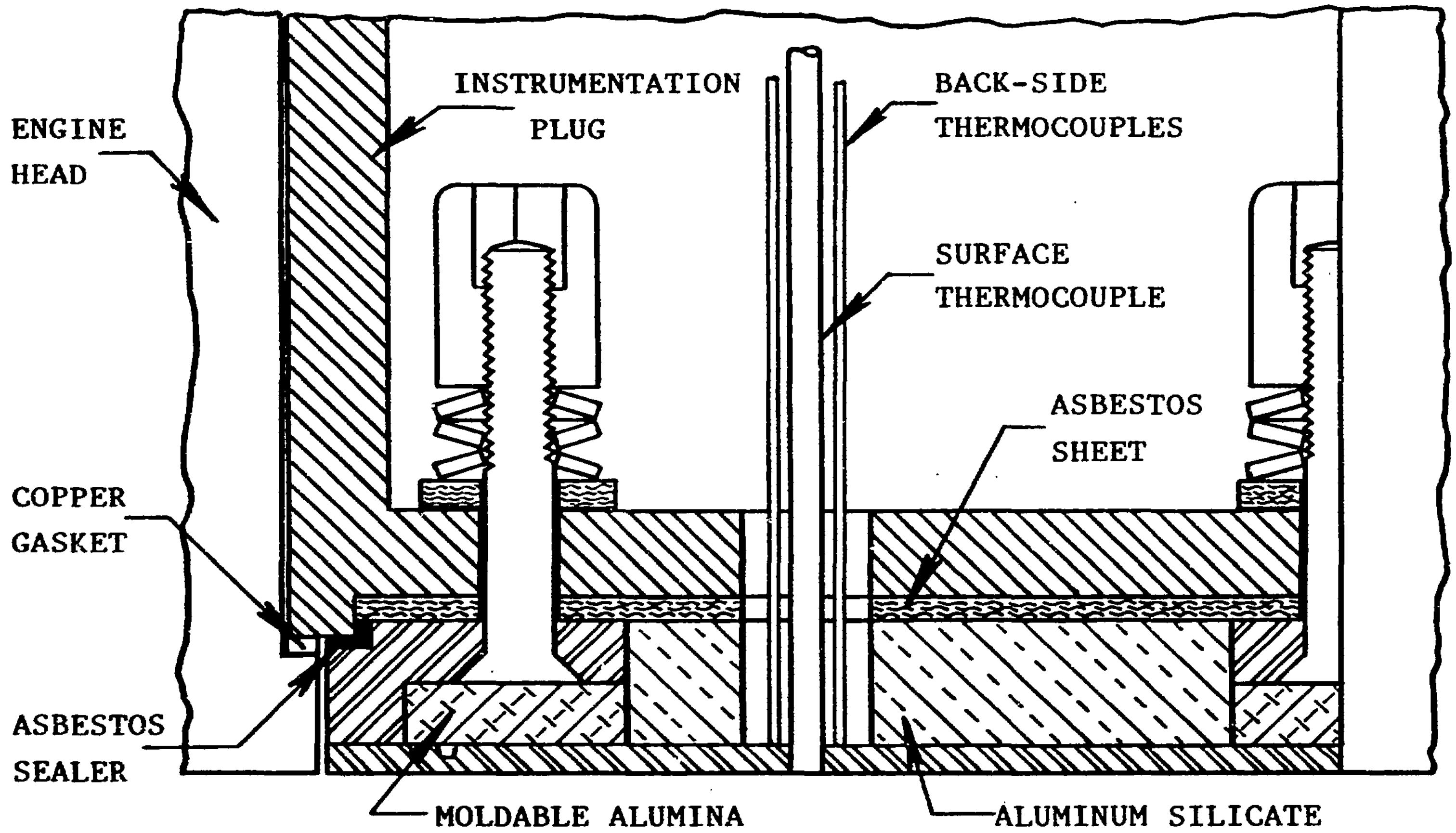

Figure 2. Insulated Instrumentation Plug Assembly with Metal Plate

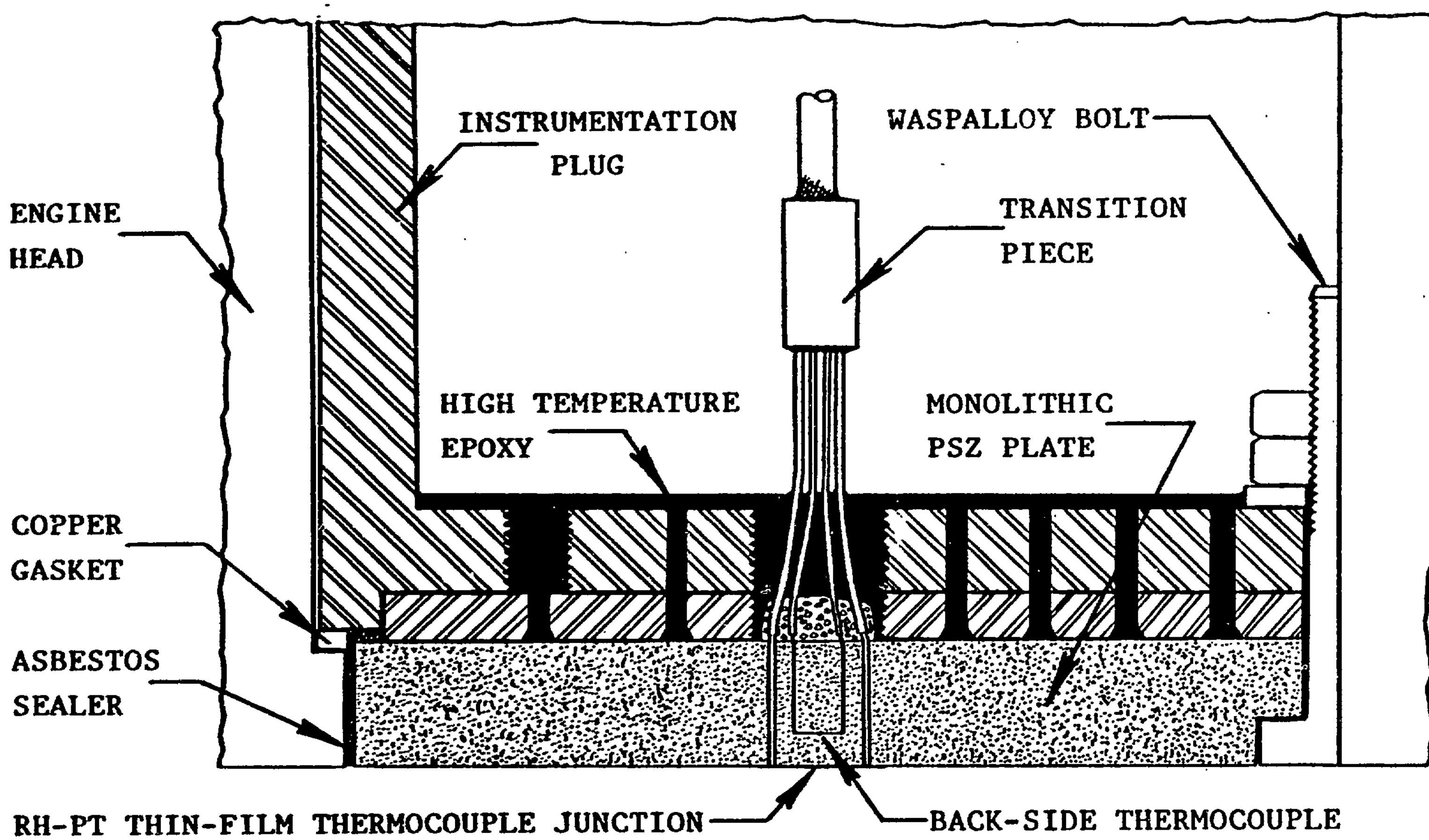

Figure 3. Insulated Instrumentation Plug Assembly with Zirconia Plate

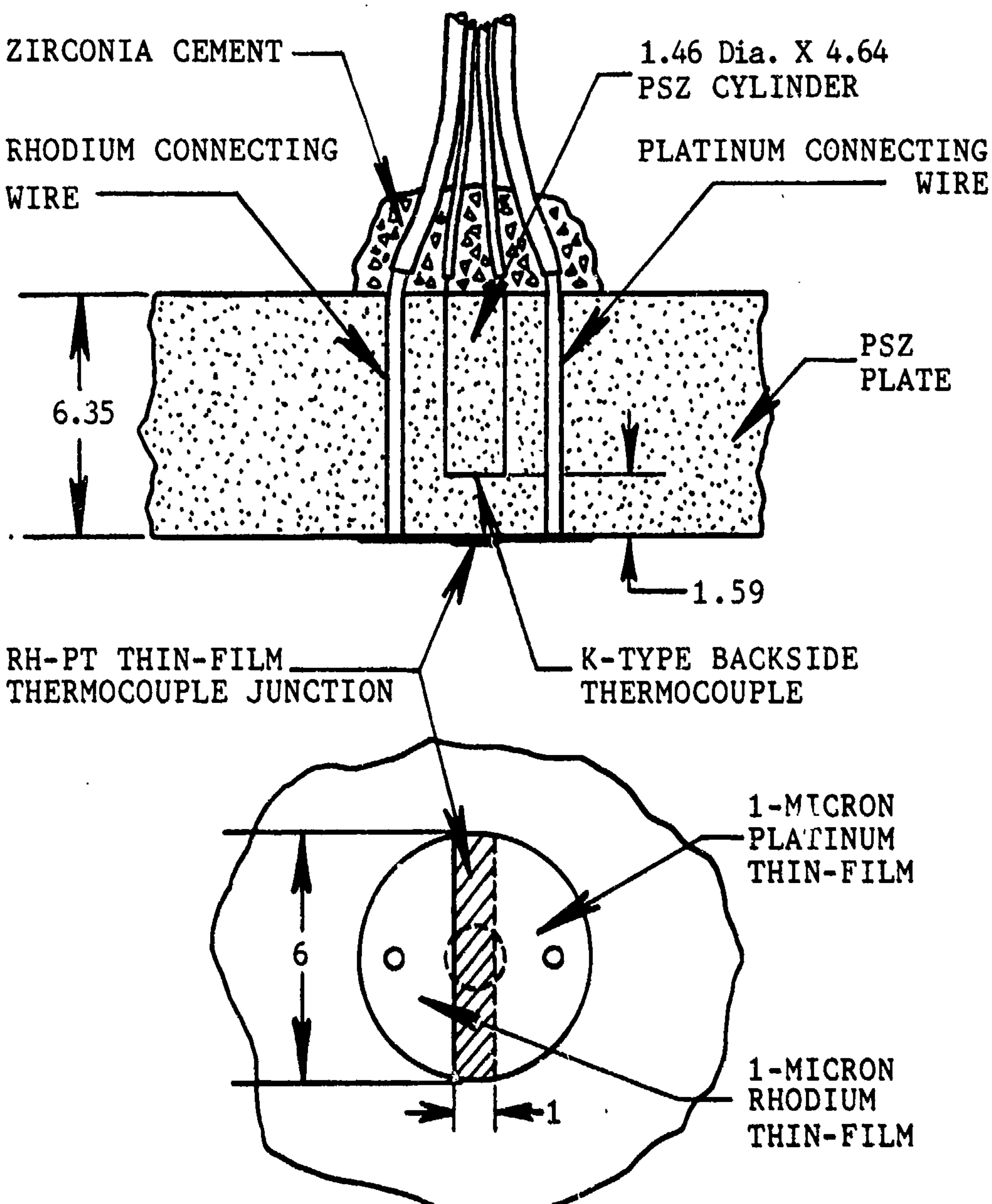

Dimensions in millimeters.

Figure 4. Rh-Pt Thin-Film Heat Flux Transducer for Zirconia Plate Plug Assembly

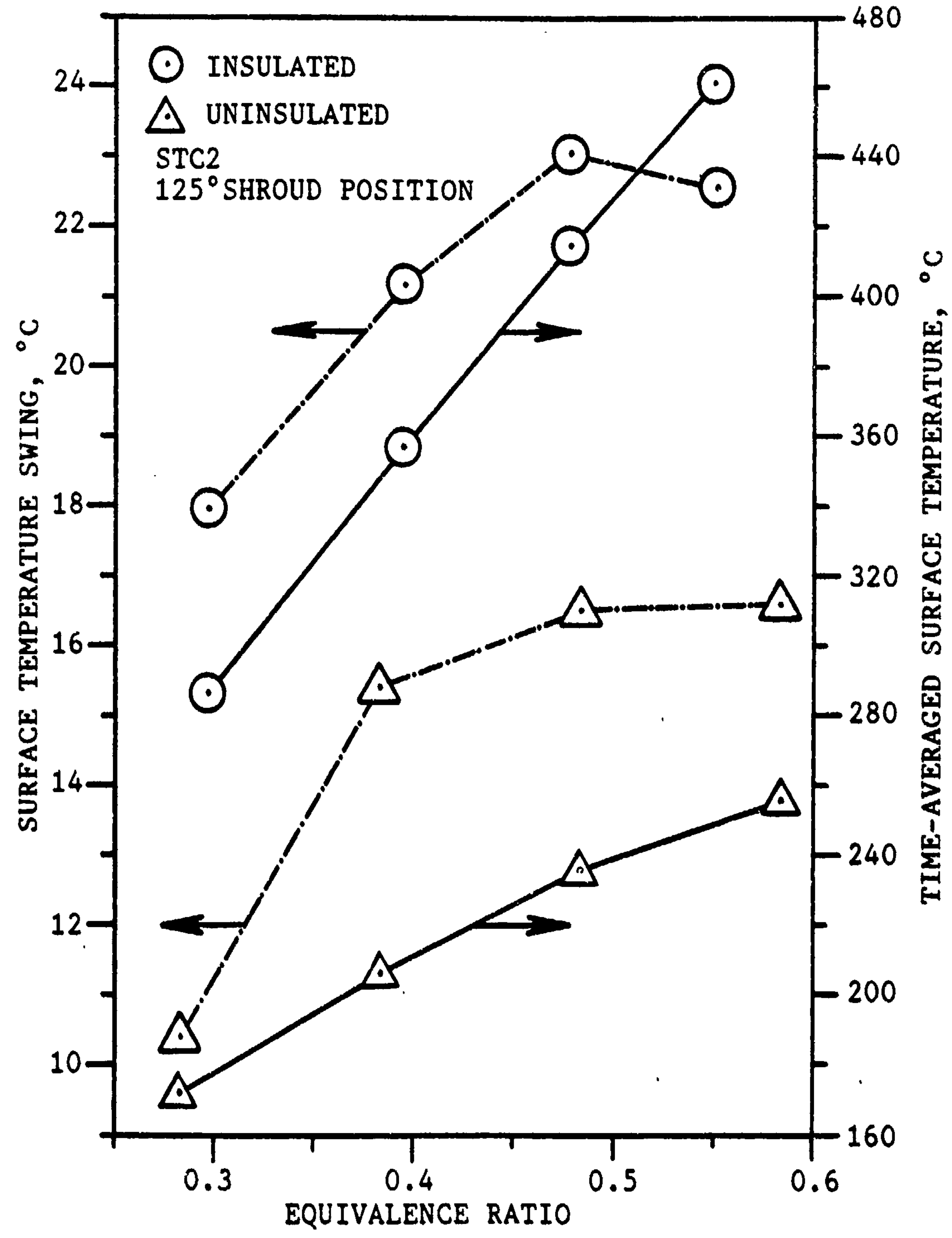

Figure 5. Time-Averaged Surface Temperature and Surface Temperature Swing versus Equivalence Ratio for the Insulated and Uninsulated Metal

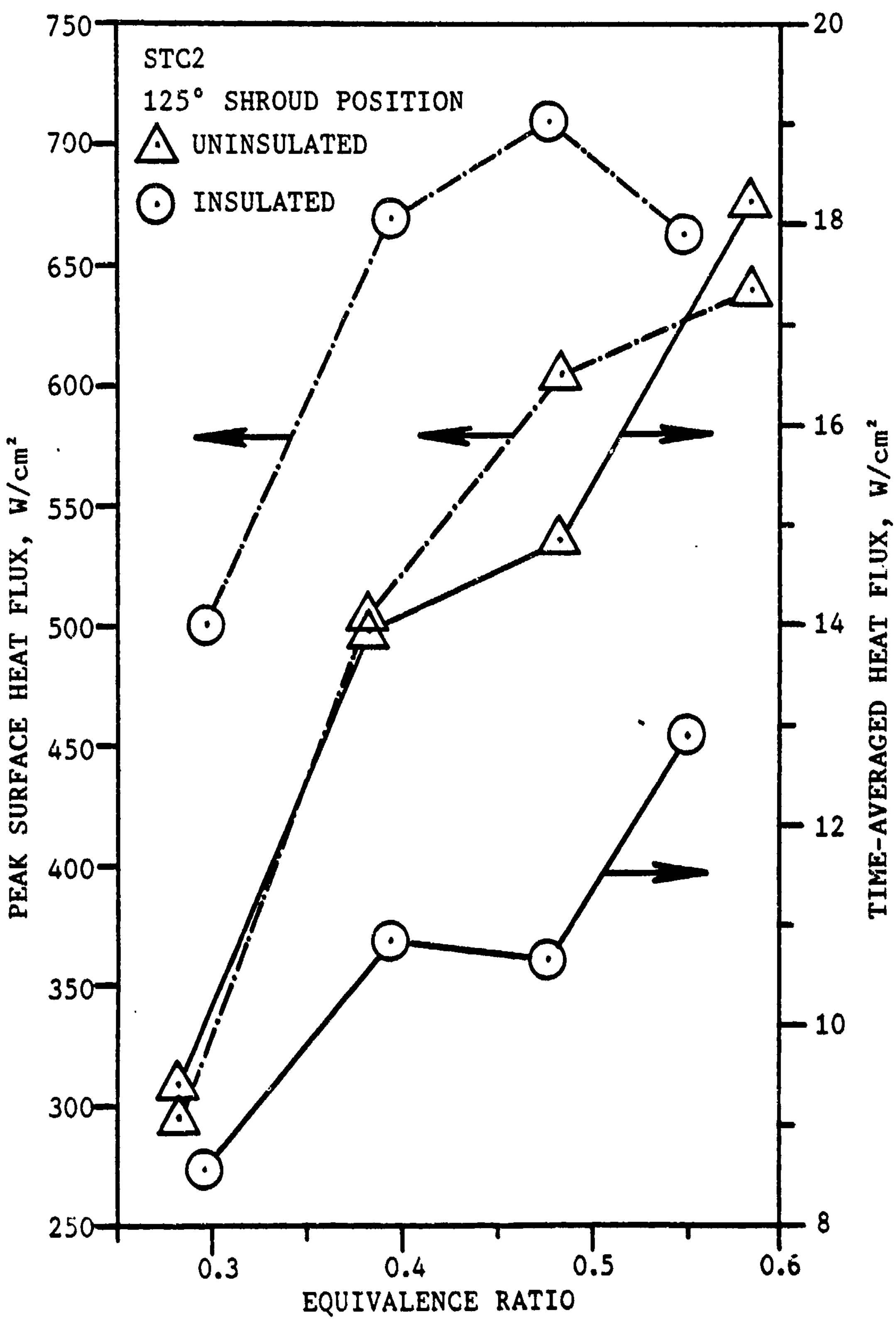

Figure 6. Peak Surface Heat Flux and Time-Averaged Heat Flux versus Equivalence Ratio for the Insulated and Uninsulated Metal

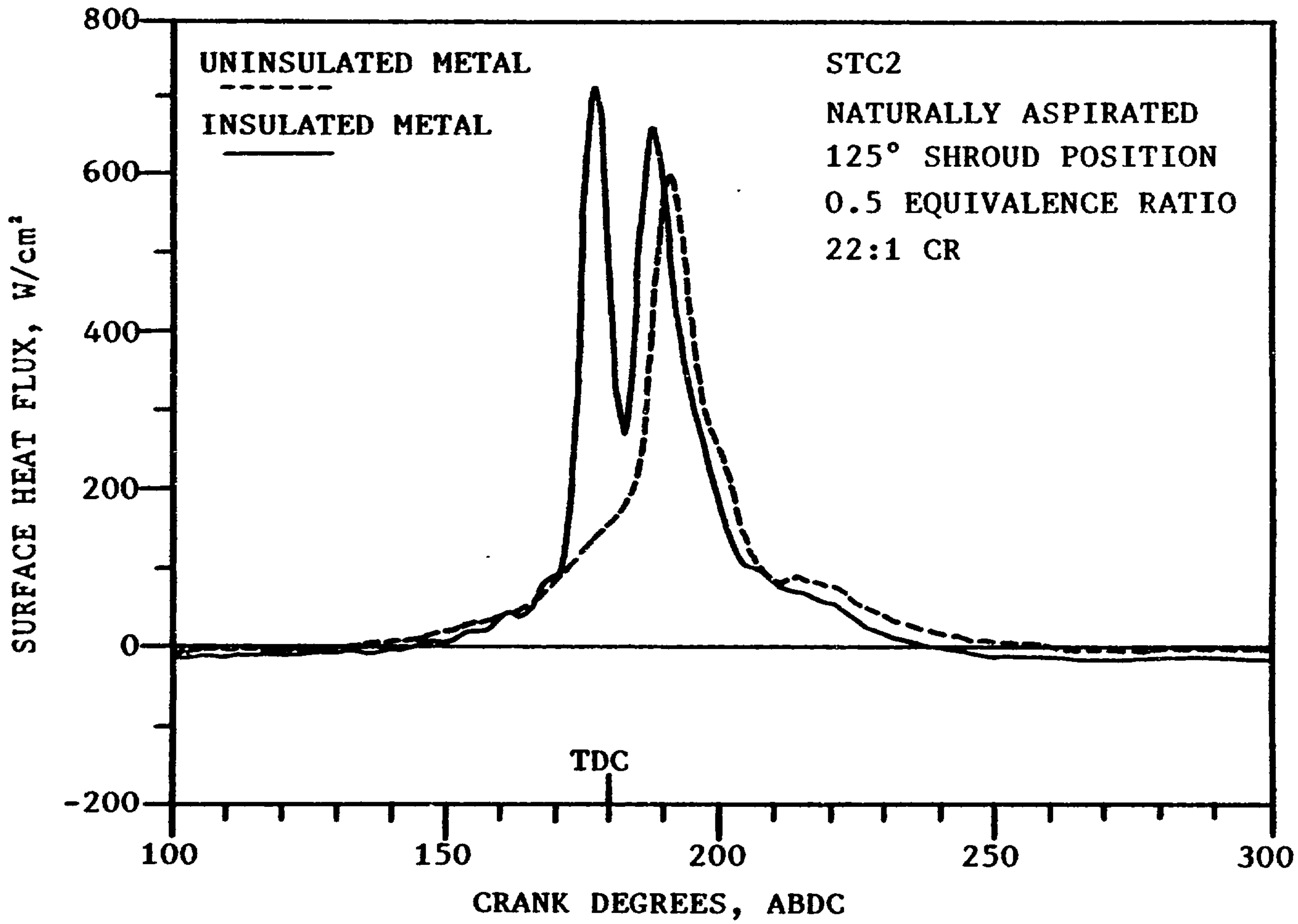

Figure 7. Comparison of Cyclic Surface Heat Fluxes for the Insulated and Uninsulated Metal

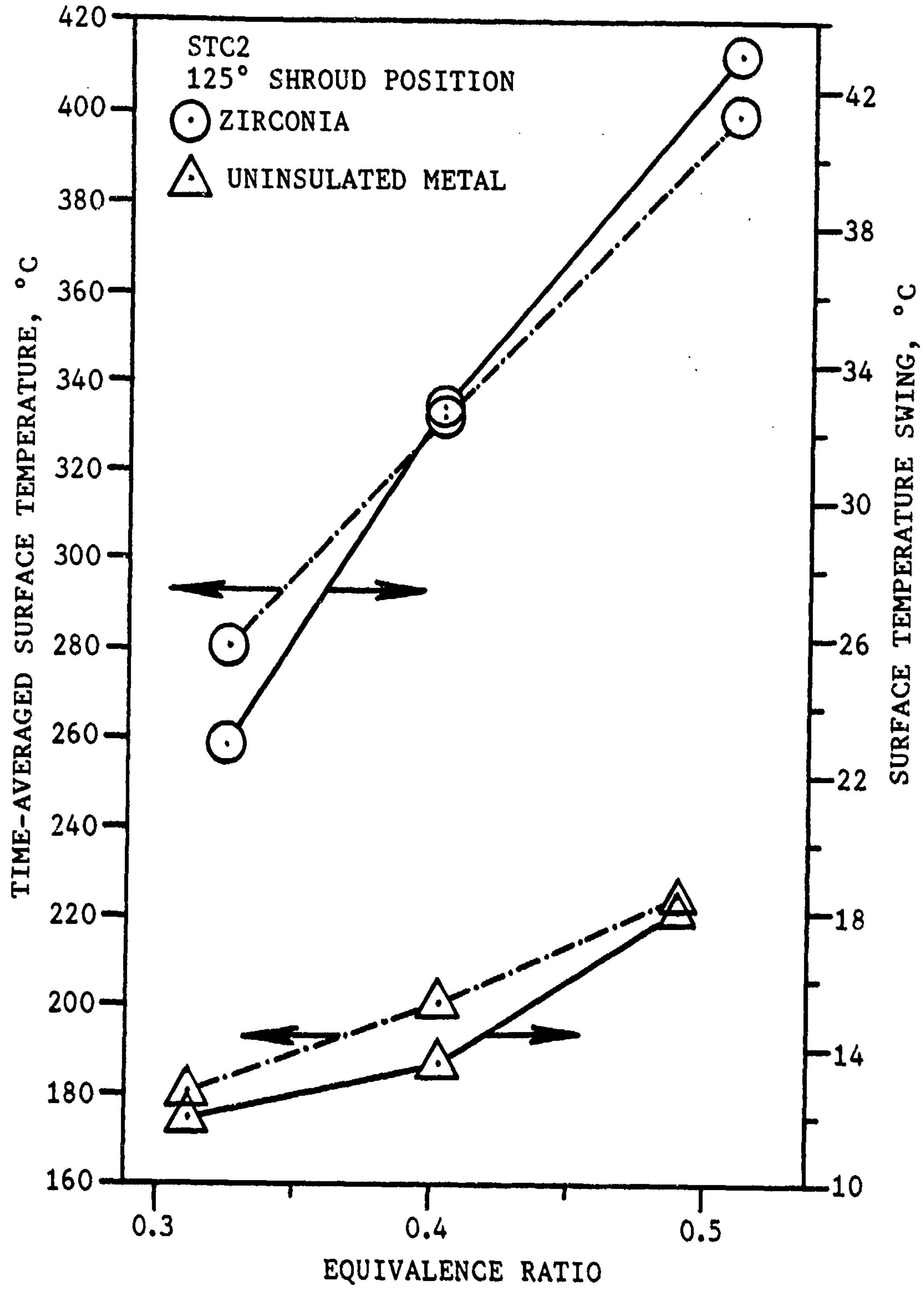

Figure 8. Time-Averaged Temperature and Surface Temperature Swing versus Equivalence Ratio for the Zirconia and Uninsulated Metal

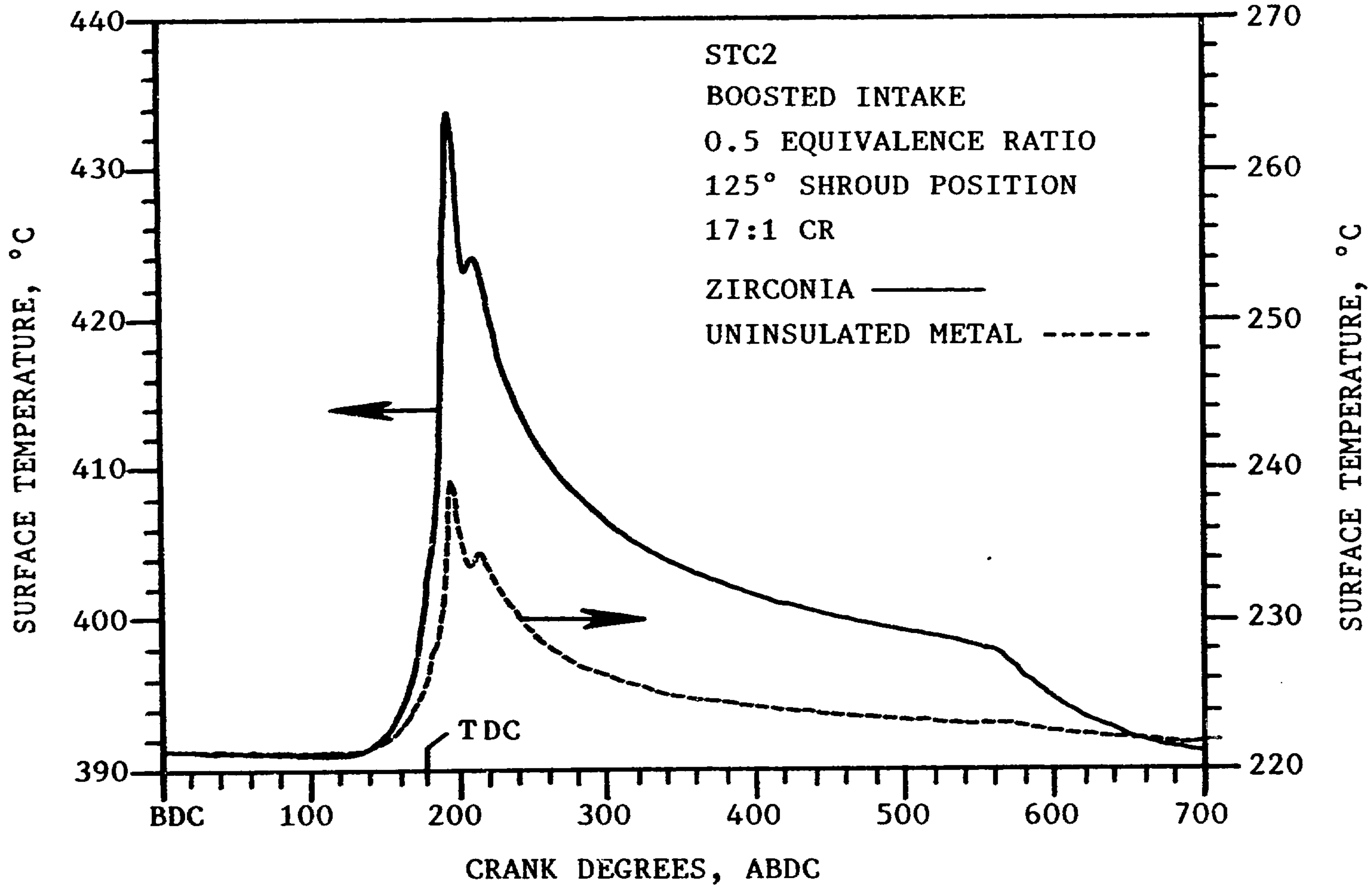

Figure 9. Comparison of Cyclic Surface Temperatures for the Zirconia and Uninsulated Metal

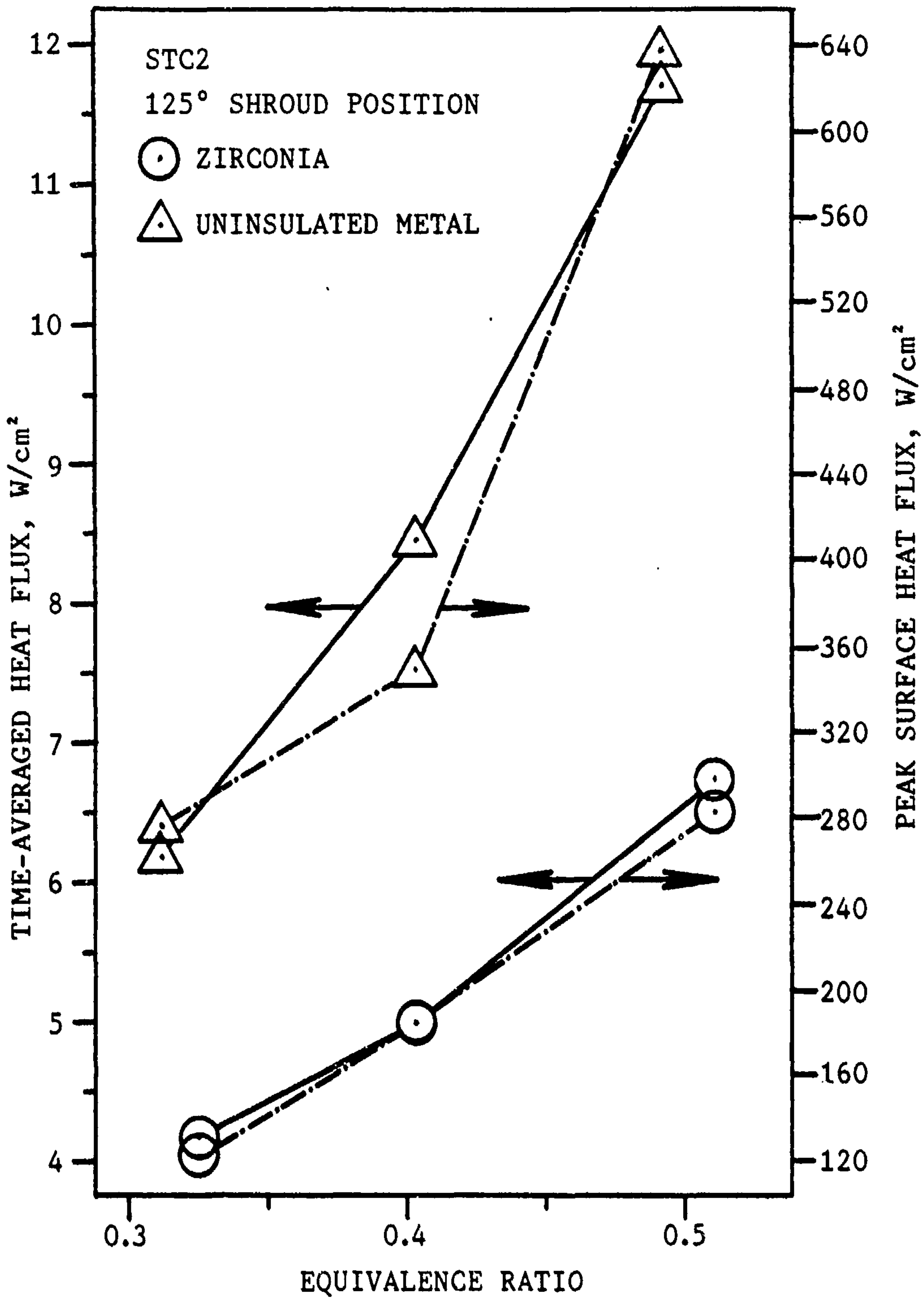

Figure 10. Peak Surface Heat Flux and Time-Averaged Heat Flux versus Equivalence Ratio for the Zirconia and Uninsulated Metal

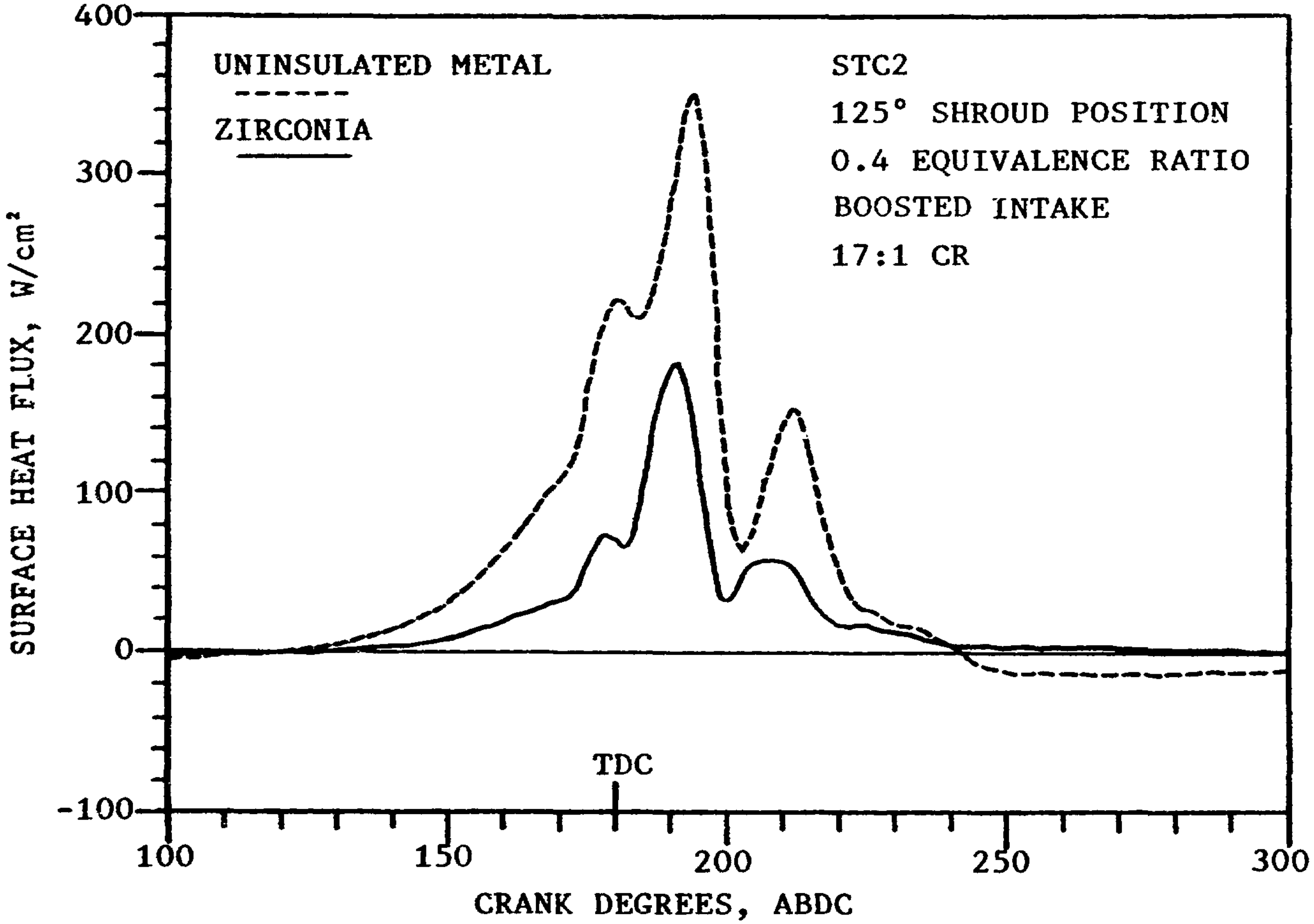

Figure 11. Comparison of Cyclic Surface Heat Fluxes for the Zirconia and Uninsulated Metal

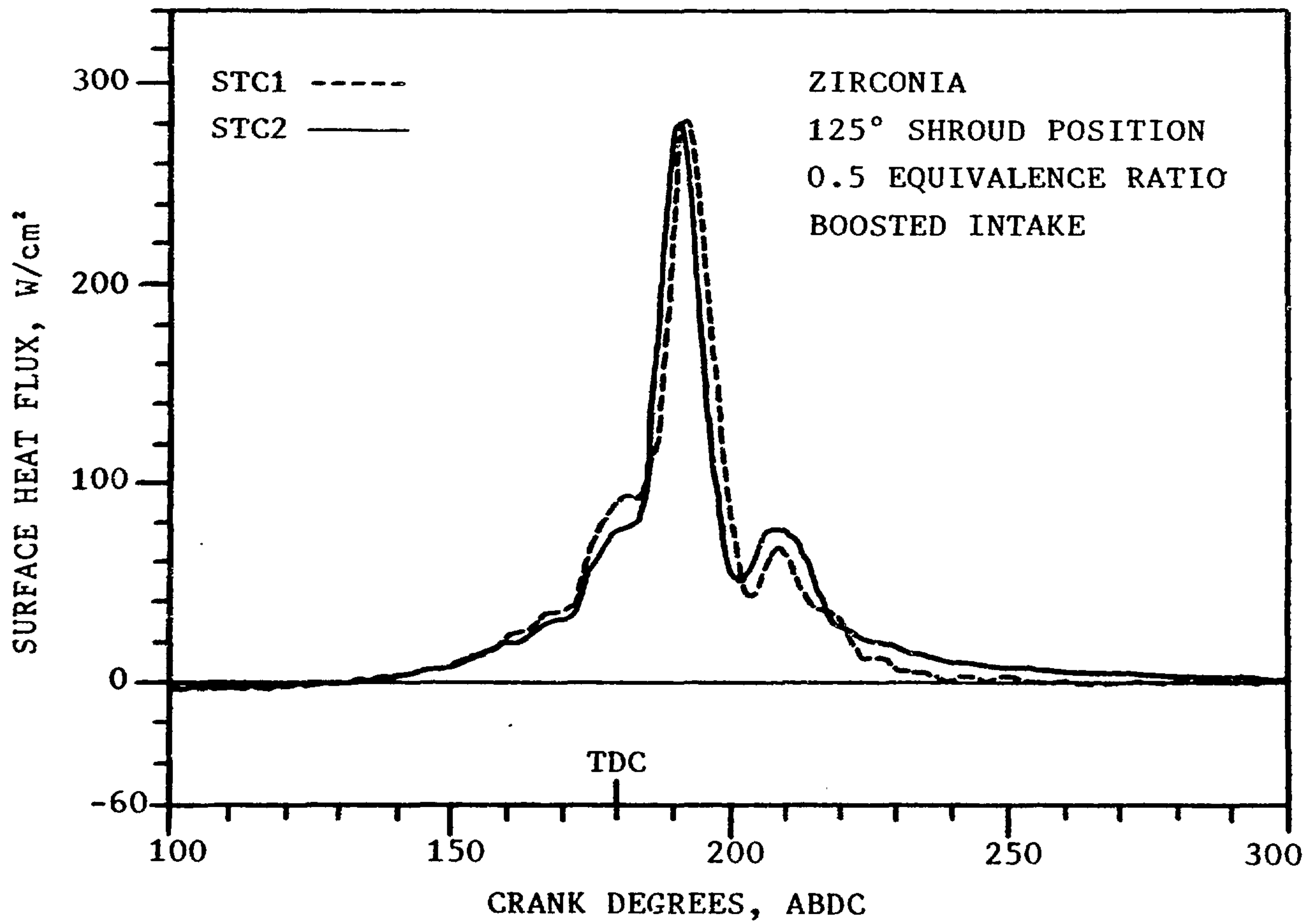

Figure 12. Comparison of Cyclic Surface Heat Fluxes at STC1 and STC2 for the Zirconia

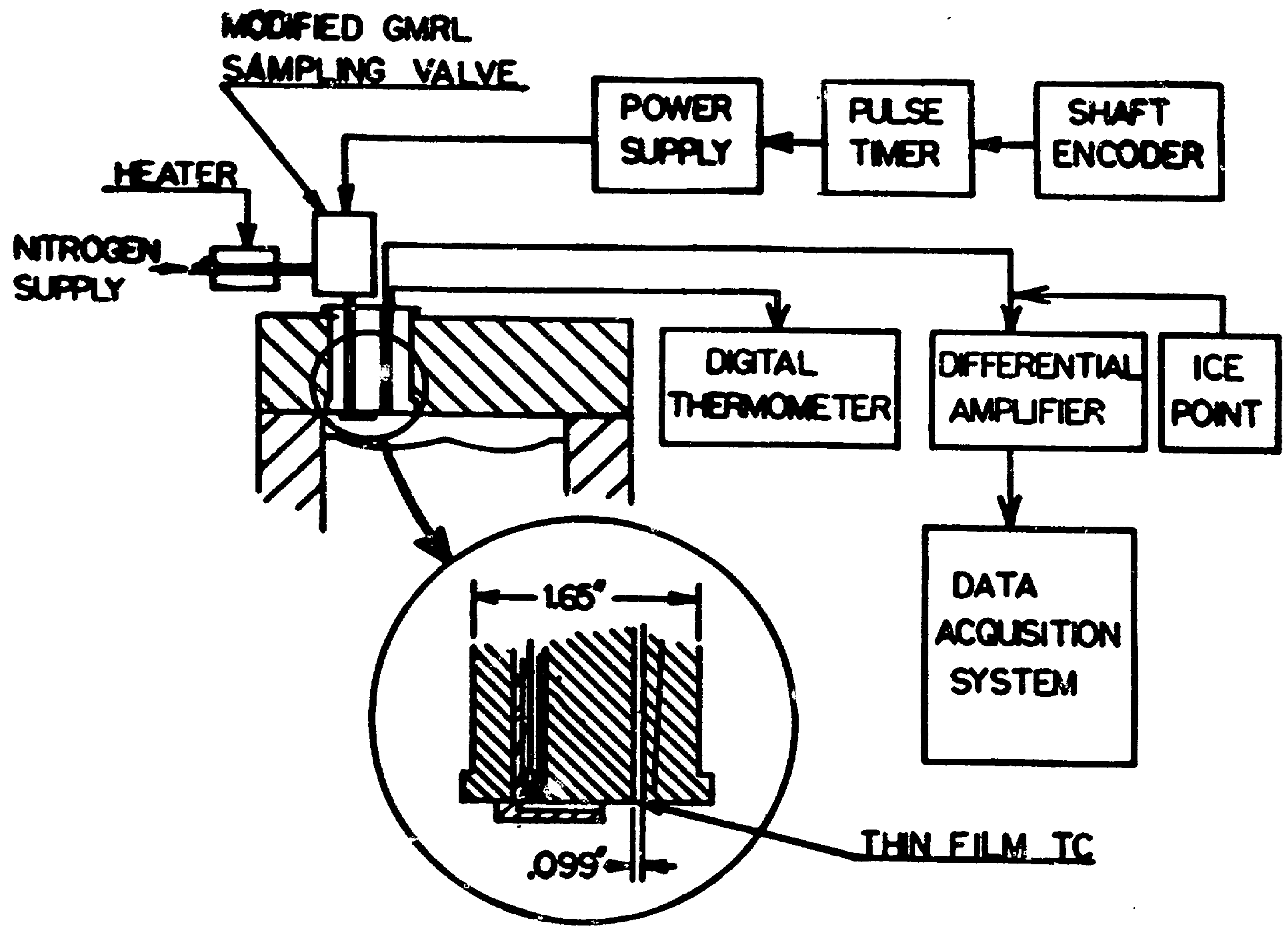

Figure 13. Schematic of Apparatus for the Wall-Jet Radiation Flux Instrument